RESEARCH ARTICLE

Structural insights into the assembly of human translesion polymerase complexes

Wei Xie[1,2], Xuan Yang[1,2], Min Xu[1] ✉, Tao Jiang[1] ✉

[1] National Laboratory of Biomacromolecules, Institute of Biophysics, Chinese Academy of Sciences, 15 Datun Road, Chaoyang District, Beijing 100101, China
[2] The Graduate University of Chinese Academy of Sciences, 19A Yuquan Road, Shijingshan District, Beijing 100039, China
✉ Correspondence: tjiang@ibp.ac.cn (T. Jiang), xumin@moon.ibp.ac.cn (M. Xu)

ABSTRACT

In addition to DNA repair pathways, cells utilize translesion DNA synthesis (TLS) to bypass DNA lesions during replication. During TLS, Y-family DNA polymerase (Polη, Polκ, Polι and Rev1) inserts specific nucleotide opposite preferred DNA lesions, and then Polζ consisting of two subunits, Rev3 and Rev7, carries out primer extension. Here, we report the complex structures of Rev3-Rev7-Rev1^{CTD} and Rev3-Rev7-Rev1^{CTD}-Polκ^{RIR}. These two structures demonstrate that Rev1^{CTD} contains separate binding sites for Polκ and Rev7. Our BIAcore experiments provide additional support for the notion that the interaction between Rev3 and Rev7 increases the affinity of Rev7 and Rev1. We also verified through FRET experiment that Rev1, Rev3, Rev7 and Polκ form a stable quaternary complex *in vivo*, thereby suggesting an efficient switching mechanism where the "inserter" polymerase can be immediately replaced by an "extender" polymerase within the same quaternary complex.

KEYWORDS   translesion DNA synthesis, Rev1, Polκ, Polζ, complex structure

INTRODUCTION

DNA lesions occurring during replication often stall the replicative DNA polymerases, block DNA synthesis and result in genome instability. One solution adopted by cells is to replace the stalled replicative DNA polymerases by specialized translesion DNA synthesis (TLS) polymerases (Goodman, 2002; Prakash et al., 2005; Lehmann et al., 2007; Guo et al., 2009;

Sale et al., 2012), which are able to replicate the DNA across the damaged site. Human TLS polymerases include four Y-family DNA polymerases (Polη, Polκ, Polι and Rev1) that exhibit high substrate flexibility, low fidelity and limited proof-reading ability (Goodman, 2002; Prakash et al., 2005; Guo et al., 2009; Sale et al., 2012), and one B-family DNA polymerase (Polζ) that consists of two protein subunits, namely Rev3 and Rev7 (Lawrence and Hinkle, 1996; Zhu and Zhang, 2003; Gan et al., 2008).

The current model of TLS has two steps as follows. In the first step, after the monoubiquitination of proliferating cell nuclear antigen (PCNA), Y-family TLS polymerases are recruited to the DNA lesions to replace the stalled replicative DNA polymerase and insert specific nucleotides opposite certain DNA lesions (Edmunds et al., 2008; Chen et al., 2010; Freudenthal et al., 2010). Polη, Polκ and Polι possess at least one Ub-binding domain (UBM or UBZ), a PCNA-interacting peptide (PIP), and a Rev1-interacting region (RIR) (Bienko et al., 2005; Plosky et al., 2006; Bomar et al., 2010). Rev1 is a multiple domain polymerase that sequentially contains an N-terminal BRCT domain that interacts with PCNA, a catalytic domain, two UBMs and a C-terminal polymerase-interacting domain (Acharya et al., 2006; Guo et al., 2006; Auerbach and Demple, 2010). Because of their Ub-binding and PCNA-interacting domains, Y-family TLS polymerases with a higher affinity for ubiquitinated PCNA assemble at the damaged template. In the second step of TLS, Y-family TLS polymerases are switched to Polζ under the regulation of Rev1, and then Polζ extends a few additional nucleotides before a replicative polymerase restarts normal DNA replication (Guo et al., 2001; Zhu and Zhang, 2003; Lehmann et al., 2007; Gan et al., 2008; Andersen et al., 2011). The C-terminal polymerase-interacting domain of Rev1 (Rev1^{CTD}) is able to

bind to the other three Y-family TLS polymerases (Guo et al., 2003; Ohashi et al., 2004; Friedberg et al., 2005; Kosarek et al., 2008; Ito et al., 2012) as well as Rev7, which is the accessory subunit of Polζ (Murakumo et al., 2001; Masuda et al., 2003; Acharya et al., 2005). Thus, Rev1^{CTD} plays a crucial role in switching Y-family TLS polymerases to B-family TLS polymerase. However, the detailed molecular mechanism is still unclear.

Polη, ι and κ interact with Rev1^{CTD} through their RIR motifs, which have been mapped by mutational analysis and multiple RIR truncations to approximately 20 residues within Polη, ι and κ (Guo et al., 2003; Ohashi et al., 2004; Kosarek et al., 2008; Guo et al., 2009; Ohashi et al., 2009). Two consecutive phenylalanines (FF) are essential and conserved in all RIRs (Ohashi et al., 2009). Regarding TLS polymerase selection, it remains unclear whether factors other than the lesion itself, such as the interactions among Rev1 and Polη, ι and κ, offer specificity for the cognate polymerase to be recruited to a specific lesion.

Rev1-Polζ complex is not only indispensible for most translesion DNA synthesis events (Shachar et al., 2009; Livneh et al., 2010) but also functions in many DNA repair pathways (Okada et al., 2005) such as DNA interstrand crosslink repair (Räschle et al., 2008) and homologous recombination repair (Sharma et al., 2011). Studies have increasingly indicated that defects in REV3 and REV1 genes are closely related to the development of tumors and the drug resistance of cancer cells (Lin et al., 2006; Dumstorf et al., 2009; Doles et al., 2010; Xie et al., 2010). Moreover, the Fanconi anemia pathway regulates translesion synthesis activity through an interaction between monoubiquitinated Rev1 and the Fanconi anemia core complex (Kim et al., 2012).

Despite a series of structures of the catalytic domain of Y-family TLS polymerases (Nair et al., 2004; Uljon et al., 2004; Nair et al., 2005; Alt et al., 2007; Biertümpfel et al., 2010) and Rev7-Rev3 structure (Hara et al., 2010) have been reported, little is known about the assembly of Rev1 with Polζ and other Y family polymerases. Here, we present the complex structures of human Rev3-7-1 and Rev3-7-1-Polκ. Our structures show that Rev1 contacts RIR motif of Polκ via a hydrophobic pocket formed by its N-terminal β-hairpin, α1, α2 helices and α1-α2 loop. In addition, we verified the details of Rev7-1 interface indicated by crystal structures using an array of pull-down assays, and confirmed the function of Rev3 in inducing and stabilizing the TLS machinery through BIAcore experiments. Moreover, a structural comparison between previous structures (Pozhidaeva A, 2012; Wojtaszek et al., 2012b) and ours show that Polη and Polκ essentially bind to Rev1^{CTD} in identical manner so that the Rev1 interaction seems to have little effect on polymerase selection. These observations, together with our FRET results, suggest that Rev1, Rev3, Rev7 and Polκ form a stable quaternary complex *in vitro* and *in vivo*, and provide comprehensive insight into TLS polymerase switching mechanism that is mediated by Rev1^{CTD} interactions.

RESULTS AND DISCUSSION

Crystal structure of the Rev3-7-1 complex

Because the free Rev1^{CTD} was susceptible to heavy degradation, it was challenging to obtain stable human Rev3-7-1 samples. Therefore, a 5(Gly-Ser)-linker sequence was introduced between full-length Rev7 and Rev1^{CTD} sequences to obtain Rev7 and Rev1 fusion protein (Rev7-Rev1^{CTD}) (Janda et al., 2010). Rev7 Arg124 was also mutated to Ala as previously reported (Hara et al., 2010). Then, Rev7-Rev1^{CTD} protein was co-expressed with the Rev7 binding domain of Rev3 (Rev3^{7BD}, residues 1847–1898), which allowed us to determine the X-ray crystal structure of the Rev3^{7BD}-Rev7-Rev1^{CTD} complex at a resolution of 2.7 Å. For simplicity, we refer to the Rev3^{7BD}-Rev7-Rev1^{CTD} complex as the Rev3-7-1 complex.

The overall structure of Rev3-7-1 shows two copies per asymmetric unit (Fig. 1A). The 5(Gly-Ser)-linker, the N-terminal 35 residues segment of Rev1, and the N-terminal 27 residues of Rev3^{7BD} are disordered and are not built into the final model. In comparison with Rev7-Rev3 complex structure reported previously (Hara et al., 2010), the Rev7-Rev3 structures present a similar conformation except that the loop between β6 and β7′ of Rev7 became visible and ordered in our structure, in which the residues 157–163 formed an α-helix named αD (Fig. 1A). The Rev1^{CTD} in the Rev3-7-1 complex is a four-helix bundle including parallel and anti-parallel helices α1 (residues 1165–1178), α2 (residues 1184–1200), α3 (residues 1203–1219) and α4 (resides 1223–1244) connected by short loops. Ahead and behind of this four-helix bundle, there are two additional regions including an N-terminal β-hairpin domain (residues 1156–1165) packing against the α1 and α2 helices and a last C-terminal 8-residue tail (Rev1^{C-tail}, residues 1244–1251) extending across the outward surface of the β8′ and β8″ sheets of Rev7.

Rev1^{CTD} binds to the Rev7 molecule at two adjacent interface regions, the C-terminal tail and the α2-α3 loop, resulting in a total buried surface area of approximately 674 Å^2 (Fig. 2A). The major part interface of Rev7 involves residues from the exposed face of β8′ and β8″ sheets, in addition to E101 from the β5 sheet and D138 from the αC-β6 loop, which form numerous hydrophilic and hydrophobic contacts with Rev1's C-tail and α2-α3 loop. In the Rev1^{C-tail}-Rev7 interface, five side chain-mediated hydrogen bonds are formed as follows: Y1244 on Rev1^{C-tail} forms two hydrogen bonds with Q200 on the β8″ sheet and E101 on the β5 sheet of Rev7, S1246 on Rev1^{C-tail} with E204 on the β8″ sheet of Rev7, K1249 on Rev1^{C-tail} with E205 on the β8″ sheet and D138 on the αC-β6 loop of Rev7; in addition, two main chain hydrogen bonds are formed between T1247 and K1249 on Rev1^{C-tail} and L186 on the β8′ sheet of Rev7; another hydrogen bond is
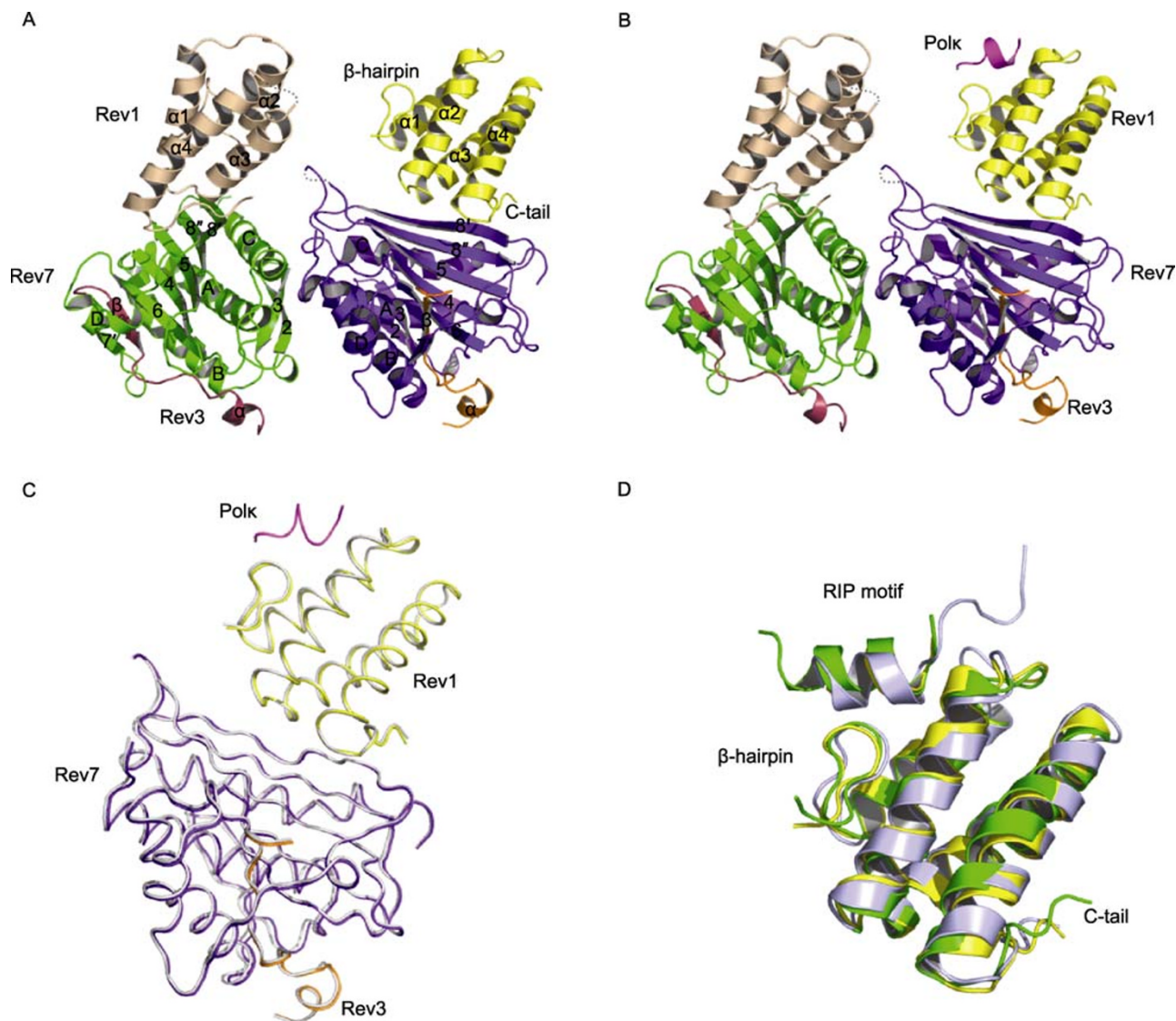
Figure 1. Overall sturctures of the Rev3-7-1 and Rev3-7-1-Polκ complexes. (A) Overall structures of the Rev3-7-1 complex. The two copies of Rev3-7-1 in the asymmetry unit are colored: Rev1 in yellow, Rev3 in orange, and Rev7 in purple blue for one copy, and Rev1 in wheat, Rev3 in green, and Rev7 in raspberry for the other copy. (B) Overall structures of the Rev3-7-1-Polκ complex. The Pol κ RIR peptide is colored in magenta. (C) Structure superposition of Rev3-7-1-Polκ and Rev3-7-1 complexes. The Rev1, Rev3, Rev7 and Polκ of the quaternary complex are colored in yellow, orange, purple blue, and magenta, respectively, and the ternary complex is colored in gray. (D) The superposition of our crystal structure of Rev1-Polκ complex and the NMR structures of human Rev1-Polη and mouse Rev1-Polκ complexes. Our crystal structure of Rev1-Polκ complex is colored in yellow, the NMR structures of human Rev1-Polη complex is colored in green, and the NMR structures of mouse Rev1-Polκ is colored in light blue. Loops not constructed in the electron density are shown as dotted lines.

formed between the main chain of Y1244 on Rev1^{C-tail} and E204 on the β8" sheet of Rev7, which make the C-tail of Rev1 tightly interact with Rev7 (Fig. 2B). In the Rev1$^{α2-α3 loop}$-Rev7 interface, D1202 and E1204 on Rev1$^{α2-α3 loop}$ form salt bridges with T191 and K190 on the β8′ sheet of Rev7, respectively; the main chain of E1200 and K1201 on Rev1$^{α2-α3 loop}$ form hydrogen bond with K198 and Q200 on the β8" sheet of Rev7, respectively; E1204 hydrogen bonds

with T191 (Fig. 2C). Moreover, besides these hydrophilic interactions, the residues L1203 on Rev1$^{α2-α3 loop}$, and Y1244 and L1248 on Rev1^{C-tail} also form hydrophobic interactions with Rev7 via residues L186, P188 and Y202 (Fig. 2D).

To further test the significance of these Rev1 sites for binding Rev7 and rule out the possibility that the linker produced artificial interacting interfaces between Rev7 and Rev1, several corresponding mutants in Rev7 including L138A,
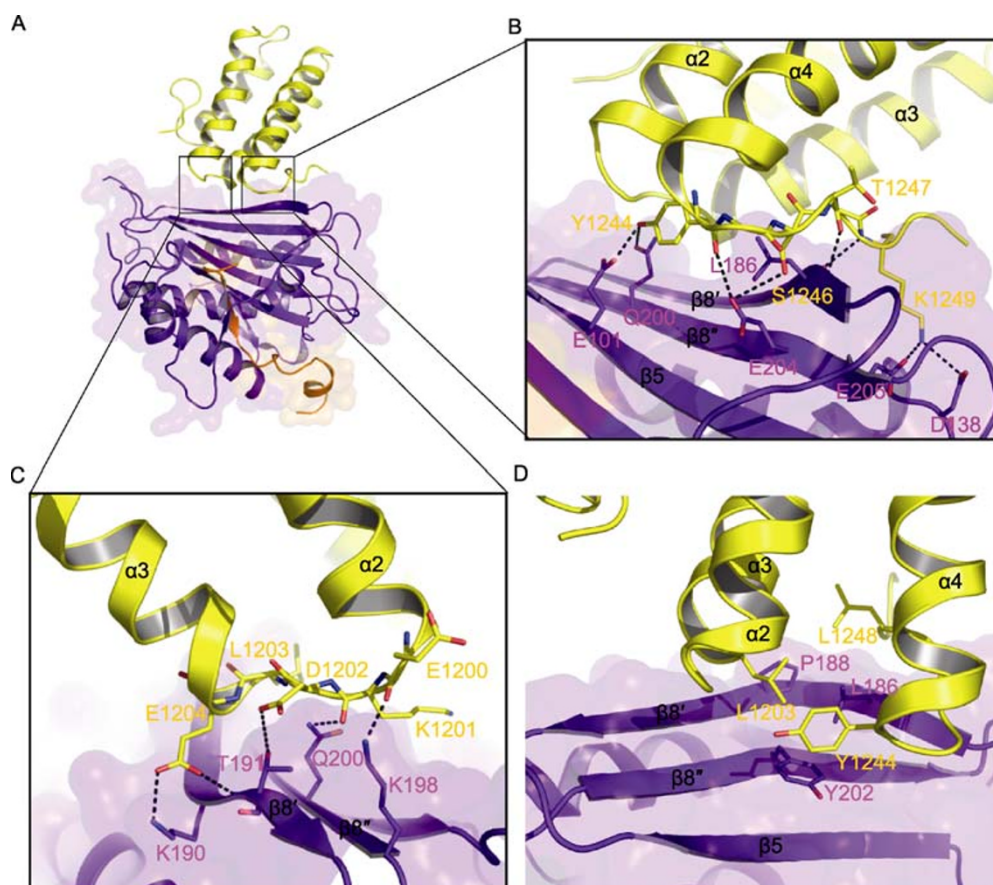
Figure 2. The Rev1-Rev7 interface. (A) The overall view of the Rev1-Rev7 interface in the Rev3-7-1 complex. (B) The hydrophilic interactions between Rev1$^{\alpha2\text{-}\alpha3\ loop}$ and Rev7. (C) The hydrophilic interactions between of Rev1$^{C\text{-}tail}$ and Rev7. (D) The hydrophobic interactions between Rev1 and Rev7. Rev1 residues are in yellow, Rev7 residues are in purple. The hydrophilic interactions are indicated by dotted lines.

K198A and E205A were performed and their bindings to GST-Rev1^{CTD} were tested. The corresponding mutants of Rev1^{CTD} including K1201A, L1203A, Y1244A, K1249A and the C-tail truncation of Rev1^{CTD} (residues 1130-1243, denoted C8) were also detected in a parallel experiment. Indeed, GST pull-down experiments show that all these mutations remarkably reduced the affinity between Rev7 and Rev1 (Fig. 3C). The pull-down results are in accordance with our structural analyses.

Function of Rev3 in forming and stabilizing the Rev3-7-1 complex

Kodai Hara et al. proposed a Rev7-Rev1 interaction model in which the binding of Rev3 to Rev7 substantially induces a conformation change of Rev7 to create a stable anti-parallel β sheets platform for contacting Rev1^{CTD} (Mapelli et al., 2007; Hara et al., 2010). Our Rev3-7-1 structure provides additional support for this model by confirming that it is the C-terminal anti-parallel β sheets the interaction region of Rev7 binding to Rev1^{CTD}. This model was further confirmed through BIAcore

experiments. Free Rev1^{CTD} was immobilized on a CM5 chip. Purified free Rev7 and Rev7-Rev3 complex were examined. Free Rev3 also flowed over immobilized Rev1^{CTD} as a negative control. BIAcore results proved that the existence of Rev3^{7BD} significantly increases the affinity between Rev7 and Rev1^{CTD} (Fig. 3A and 3B), indicating that Rev3 plays a critical role in forming and stabilizing the Rev3-7-1 complex. The requirement of Rev3 to stabilize the Rev1-binding conformation of Rev7 ensures that Rev7 and Rev3 have to be assembled to form a complete Polζ before being recruited by Rev1^{CTD} to the DNA lesion site.

Crystal structure of Rev3-7-1-Polκ

To create the complex of Rev3-7-1 with Polκ^{RIR} motif, custom synthesized 10-aa RIR peptide of Polκ was added into hanging drops to soak the crystals overnight prior to data collection. Finally, we obtained the crystal structure of the Rev3-7-1 in complex with Polκ^{RIR} which we named the Rev3-7-1-Polκ complex, at a resolution of 3.2 Å.

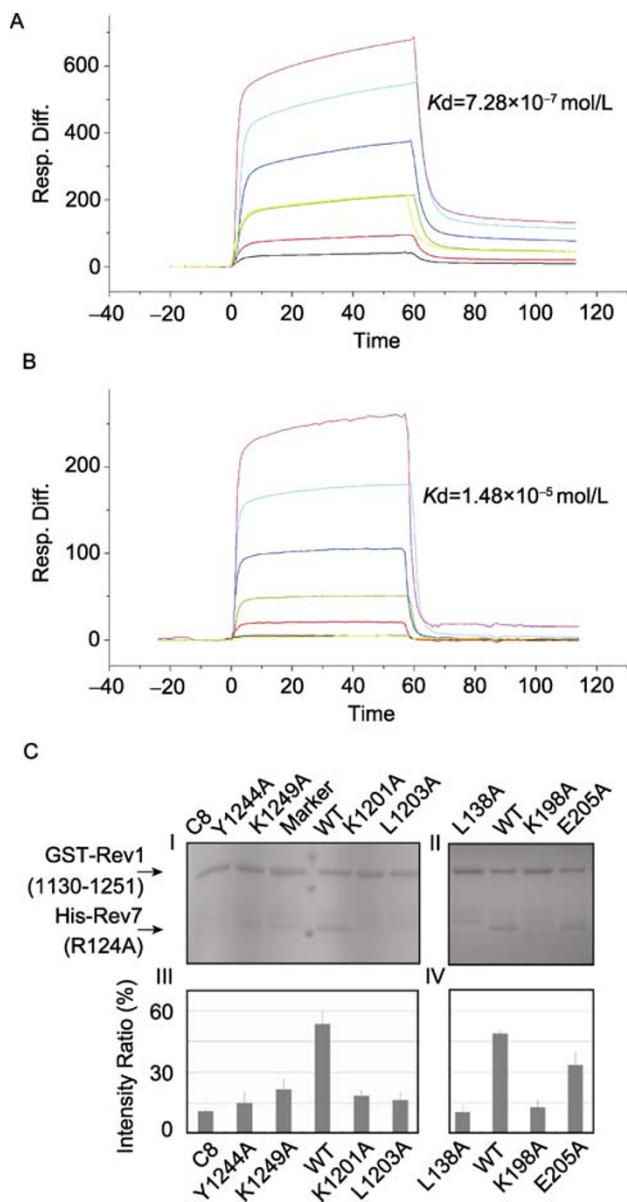**Figure 3. BIAcore analyses of the Rev7-Rev3 complex and free Rev7 binding to Rev1^CTD and pull-down assays of Rev1^CTD and Rev7-Rev3 complex.** (A) Binding of 50–1600 nmol/L Rev7-Rev3 complex to immobilized Rev1^CTD. (B) Binding of 0.4–12.8 μmol/L free Rev7 to immobilized Rev1^CTD. For both binding assays shown in (A) and (B), the concentration of 400 nmol/L was repeated as an internal control, the data are expressed as the signal obtained using each concentration and analyzed using BIAevaluation 4.1 and Origin. The calculated K values are indicated. (C) GST pull-down assays of Rev1^CTD and Rev7-Rev3 complex. Coomassieblue-stained SDS-PAGE was shown in panel I and II. The ratios of band intensities of Rev7 to band intensities of GST-Rev1^CTD were calculated with ImageJ and values were averaged and the S.E.M. was calculated, which were shown in panel III and IV. Panel I and III show the wide type (WT) and mutants of Rev1^CTD, and the WT and mutants of Rev7 are shown in panel II and IV.

In the Rev3-7-1-Polκ complex, only one of the two Polκ^RIR had ordered electron density and residues spanning 566-572 was constructed into the final model. Residues L1159, A1160 on the N-terminal β-hairpin, L1171, W1175, D1186, V1190 on the α1, α2 helices and I1179, P1182, M1183 on the α1-α2 loop create a large hydrophobic pocket on Rev1^CTD, embracing the two conserved Phe residues (F567, F568) of Polκ RIR peptide which folds into an α-helix upon binding (Fig. 1B). Structure superposition of the Polκ RIR peptide-bound and unbound Rev3-7-1 complex reveals no noticeable structural changes (Fig. 1C), which suggests that binding of RIR motif does not affect the conformation of the Rev3-7-1 complex, and the N-terminal β-hairpin of Rev1^CTD is already folded into a stable structure without binding to the Polκ RIR motif. Furthermore, according to crystal structure analyses, we found that there is no noticeable contact between the N-terminal β-hairpin of Rev1^CTD and the neighboring symmetry molecules (Fig. 4B and 4C), indicating that the formation of the N-terminal β-hairpin of Rev1^CTD is not forced by crystal packing.

Very recently, Wojtaszek et al and Pozhidaeva et al presented NMR structures of mouse Rev1^CTD-Polκ^RIR and human Rev1^CTD-Polη^RIR (Pozhidaeva A, 2012; Wojtaszek et al., 2012b), respectively. Compared with our crystal structures, Polη and Polκ share the same binding region involving the N-terminal β-hairpin, α1, α2 helices and α1-α2 loop of Rev1^CTD, indicating that Polη, ι and κ compete to bind to Rev1 in DNA lesion sites (Fig. 1D). Notably, Rev7 and RIR motifs of Y-family polymerases interact with Rev1 in diagonal positions; meanwhile, the interacting region of Rev1 and Polκ locate opposite to that of Rev1 and Rev7, which leads to minimize steric hindrance considering the large size of these TLS polymerases.

Rev1, 3, 7 and Polκ form a stable quaternary complex in vivo

To confirm the results from the pull-down experiments and crystal structures, formation of Rev3-7-1-Polκ complex *in vivo* was further characterized using FRET experiment. HEK-293T cells were co-transfected with pcDNA^Rev3 and Rev7-mKO and pcDNA^Rev1 and Polκ-EGFP as well as pcDNA^Rev3 and Rev7-mKO and pcDNA^PolκRIR-EGFP, which only differs on the expression of Rev1^CTD. As shown in Fig. 5A, the intensity of Polκ-EGFP fluorescence was determined by both pre- and post- photobleaching of Rev7-mKO. With the expression of Rev1^CTD, photobleaching of Rev7-mKO significantly increased the fluorescence intensity of Polκ-EGFP, thereby indicating robust FRET between these two proteins (Fig. 5A and 5B). By contrast, in the absence of Rev1^CTD, the fluorescence intensity of Polκ-EGFP was not significantly increased after the photobleaching of Rev7-mKO (Fig. 5B), which suggests that Rev7 and Polκ do not directly interact with each other. Therefore, it is the co-expression of Rev1^CTD that leads to the
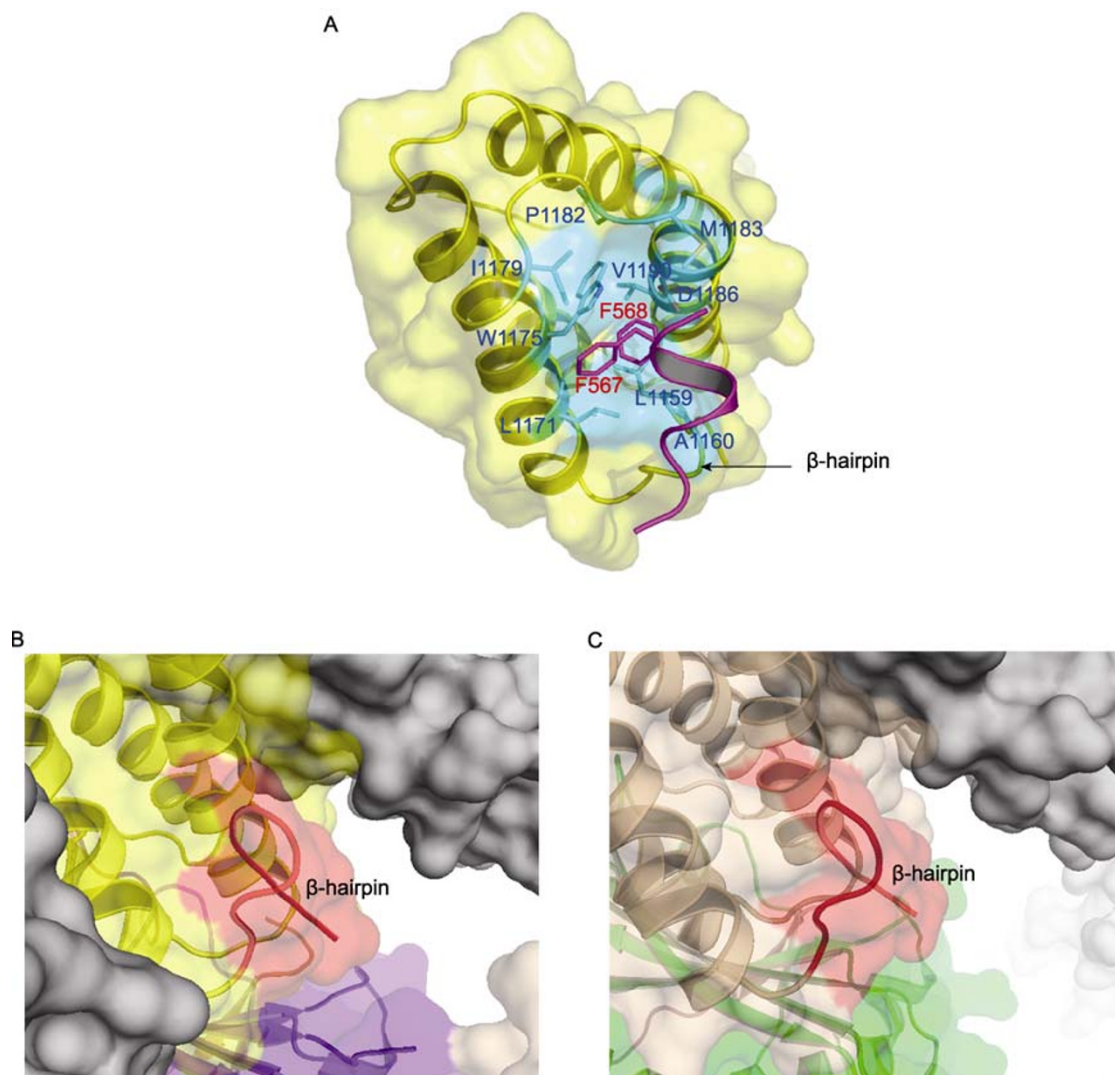
Figure 4.   The Rev1-Polκ interface. (A) The hydrophobic pocket formed by N-terminal β-hairpin, α1, α2 helices and the α1-α2 loop of Rev1[CTD], responsible for the RIR motif binding. Rev1 is colored in yellow, and the residues of the hydrophobic pocket are colored in cyan. Polκ is colored in magenta with the two Phe residues shown in stick. (B and C) The N-terminal β-hairpin of Rev1[CTD] and the neighboring symmetry molecules. The two copies of Rev3-7-1 shown as cartoon and surface in the asymmetry unit are colored: Rev1 in yellow, Rev3 in orange, and Rev7 in purple blue for on copy, and Rev1 in wheat, Rev3 in green, and Rev7 in raspberry for the other copy. Both of the two N-terminal β-hairpins in the asymmetry unit are highlighted in red. The symmetry molecules are shown as surface and colored in gray.

increased FRET signals between Rev7-mKO and Polκ-EFGP , indicating that Rev1[CTD] serves as a bridge to assemble Rev7 and Polκ[RIR]. Based on our data, Rev3-bound Rev7 and Polκ are able to bind to Rev1 simultaneously to form a stable quaternary complex *in vivo*, and other types of Y-family TLS polymerases may also assemble into a stable quaternary complex with Rev3-7-1 in a similar manner.

Mechanism of Y-family TLS polymerases switch to Polζ bridged by Rev1[CTD]

Upon encountering a damage template, the normal replica-

tion machinery stalls at the DNA lesion site, which results in PCNA monoubiquitination that is catalyzed by the Rad6-Rad18 complex (Hoege et al., 2002). Monoubiquitinated PCNA recruits Rev1 and other Y-family TLS polymerases to the damage site (Hoege et al., 2002; Garg et al., 2005; Edmunds et al., 2008; Freudenthal et al., 2010). It has been shown that Rev1 and other Y-family TLS polymerase could been recruited independently (Ito et al., 2012). Meanwhile, Polζ, as a whole, also assembles at the damage site through the interaction between Rev7 and Rev1. As a result, Polζ, Rev1 and Polκ simultaneously assemble to form the stable translesion synthesis machinery, where Rev1 func-
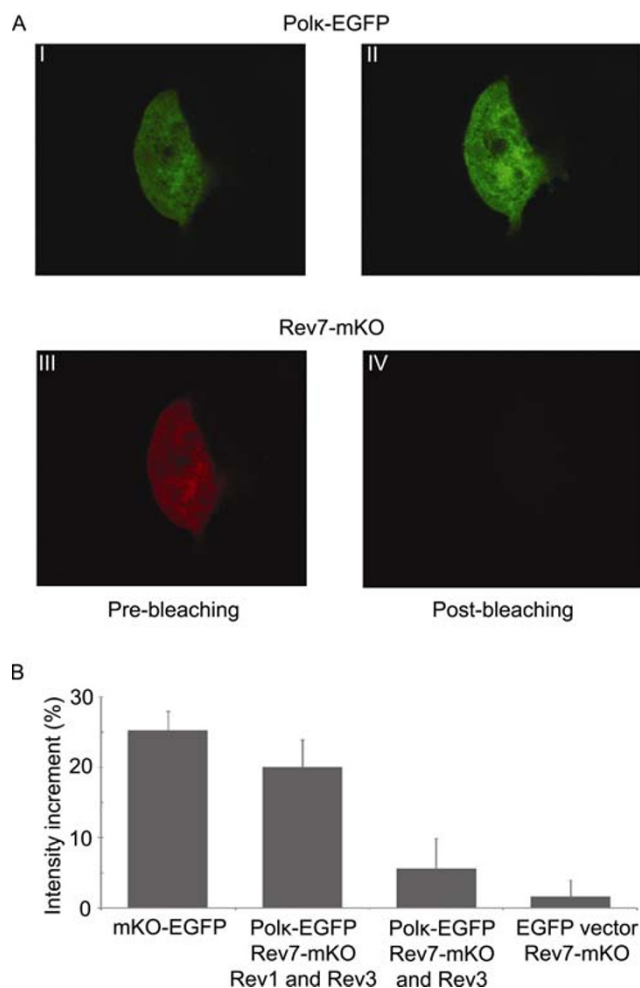
Figure 5. *In vivo* **FRET of Polκ-EGFP and Rev7-mKO.** (A) Cellular images acquired of a HEK293T cell expressing Polκ-EGFP and Rev7-mKO. Panel I and II show the Polκ-EGFP-fluorescence before and after 4 min of acceptor photobleaching, respectively. Panel III and IV show the Rev7-mKO-fluorescence before and after 4 minutes of acceptor photobleaching, respectively. Clearly, the photobleaching of Rev7-mKO increased the fluorescence intensity of Polκ-EGFP. (B) Intensity increment of Polκ-EGFP-fluorescence. Mean fluorescence intensity data are derived from whole cell regions of interest using ImageJ. Data from different cells (cell number > 20) were averaged and the S.E.M. was calculated.

tions as a bridging scaffold. After Y-family polymerase bypasses a number of specific DNA lesions, Polκ is easily replaced by Polζ for the primer extension by the TLS machinery complex mediated by the interaction with Rev1^{CTD}. In summary, in light of our structural and functional studies, we propose a model of TLS polymerases switching mechanism. This model emphasizes that the "inserter" and "extender" TLS polymerases are loaded together into TLS machinery to facilitate nucleotide insertion and extension as required. When the insertion is completed, the "inserter" polymerase is immediately replaced by the "extender" polymerase in the same complex with Rev1 and may not be required to be stripped from Rev1.

MATERIALS AND METHODS

Protein expression, purification, and crystallization

A sequence encoding a Rev7 and Rev1 fusion protein encompassing full-length human Rev7 with an R124A mutation, 5(Gly-Ser)-linker, and the last 135 amino acids of human Rev1 (Rev1^{CTD}, residues 1117–1251) was constructed into the MCS1 of pETDuet-1 plasmid with an N-terminal His-tag. A sequence encoding human Rev3 fragment (Rev3^{7BD}, residues 1847–1898) was cloned into the MCS2 of the same plasmid and coexpressed with Rev7-1^{CTD} protein in *Escherichia coli* BL21 (DE3) cells. To purify the Rev3-7-1 complex, the cells were lysed using French press in buffer A containing 50 mmol/L Tris-HCl at pH 8.0, 0.3 mol/L NaCl, 20 mmol/L imidazole, 1 mmol/L PMSF and 0.5% Triton X-100. The ternary complex was purified by Ni-NTA-affinity chromatography (GE Healthcare) and dialyzed to buffer B (20 mmol/L Tris-HCl at pH 8.0, 30 mmol/L NaCl, 5 mmol/L DTT), and then sequentially purified on a Resource Q column and a Superdex 200 gel filtration column (GE Healthcare) in buffer C (20 mmol/L Tris-HCl at pH 8.0, 100 mmol/L NaCl, 5 mmol/L DTT). The eluted fractions were analyzed by SDS-PAGE, and highly purified fractions were pooled and concentrated to ~15 mg/mL for crystallization screening (Hampton Company). The complex crystals were crystallized in 0.1 mol/L sodium citrate at pH 5.8, 1.95 mol/L sodium formate, 20 mmol/L DTT by hanging-drop vapor diffusion at 16°C, and improved by the micro-seeding method.

To obtain the Rev3-7-1-Polκ complex, a custom synthesized 10-aa peptide (KKSFFDKKRS) of the RIR region of Polκ was dissolved in Buffer C at a concentration of 10 mg/mL and added into the hanging drop at a ratio of 1:10 to soak the crystals overnight prior to data collection.

X-ray data collection and structure determination

The diffraction data sets were collected at of Shanghai Synchrotron Radiation Facility (SSRF), on beamline BL17U and processed with HKL2000 software (Otwinowski and Minor, 1997). The crystal belonged to the P2$_1$2$_1$2 space group with two copies of the Rev3-7-1 complex per asymmetric unit. The structure was solved by molecular replacement using Molrep of the CCP4 program suite (1994), with the Rev7-Rev3 heterodimer structure (Protein Data Bank [PDB] ID: 3ABD) as the search model (Hara et al., 2010). The resultant high-quality electron density map allows unambiguous building of the Rev1 model. The Rev3-7-1-Polκ structure was solved with the resulting Rev3-7-1 structure as the search model. Model building was performed with Coot (Emsley and Cowtan, 2004) and refinement was carried out using Refmac (Murshudov et al., 1997) and PHENIX (Adams et al., 2010). Data collection and refinement statistics are shown in Table 1. Structure figures were prepared using PyMol (http://www.pymol.org), and the coordinates were deposited in PDB under accession code 4GK0 and 4GK5.

Table 1 Data collection and refinement statistics

	Rev3-7-1	Rev3-7-1-Polκ
Data collection		
Wavelength (Å)	0.9791	0.9795
Resolution (Å)	20–2.7 (2.8–2.7)	20–3.2 (3.31–3.2)
Space group	$P2_12_12$	$P2_12_12$
Cell dimensions		
a, b, c (Å)	121.09, 71.89, 106.31	120.00, 72.76, 104.65
α, β, γ (°)	90, 90, 90	90, 90, 90
Unique reflections	25,137(2511)	14,598 (1531)
I/σ (I)	22.3 (3.3)	21.5 (5.2)
Completeness (%)	95.9 (97.5)	100 (100)
R_{merge} (%)[a]	6.3 (38.3)	8.7 (43.1)
Refinement		
$R_{working}$ (%)[b]	21.8	23.2
R_{free} (%)[c]	27.3	28.1
Average B factor (Å)	52.34	52.38
rmsd bounds (Å)	0.011	0.011
rmsd angles (°)	1.554	1.626

Numbers in parentheses represent statistics for the highest resolution shell.

[a] $R_{merge} = \sum |I - <I>| / \sum I$, where I is the measured intensity for reflections with indices *hkl*.

[b] $R_{working} = \sum ||F_{obs}| - |F_{calc}|| / \sum |F_{obs}|$.

[c] R_{free} = R factor for a selected subset (10%) of the reflections that were not included in prior refinement calculations.

In vitro pull-down assays

His-tagged wild-type and mutant Rev7-Rev3[7BD] complex were co-expressed as previously described (Hara et al., 2010). Wild-type and mutant Rev1[CTD] (residues 1130–1251) were subcloned into pGEX6p-1 plasmid to produce GST-Rev1[CTD] proteins. All of the proteins were overexpressed in *Escherichia coli* BL21 (DE3). The *in vitro* binding assays were performed according to standard procedure. Briefly, wild-type or mutant GST-Rev1[CTD] -bound glutathione-sepharose beads were incubated with mutant or wild-type Rev7-Rev3 complexes in buffer D (20 mmol/L HEPES at pH 7.5, 150 mmol/L NaCl, 1 mmol/L DTT) for 2 h at 4°C. Protein-bound glutathione resins were washed five times using binding buffer D, and the bound samples were analyzed using Coomassieblue-stained SDS-PAGE. Pull-down assays were repeated three times and data were calculated using ImageJ (National Institute of Health).

BIAcore experiments

Interactions of Rev1[CTD] with Rev7 and Rev7-Rev3[7BD] were measured on a BIAcore 3000 instrument (BIAcore AB, Uppsala, Sweden). Free Rev1[CTD] (residues 1130–1251) was prepared by removing the GST-tag of GST-Rev1[CTD] (residues 1130–1251) using prescission protease cleavage, followed by protein purification on a Superdex200 sizing column (GE Healthcare). Rev1[CTD] was immobilized on the carboxymethylated dextran surface-modified chip (CM5 chip) in accordance with the amine-coupling protocol of the BIAcore manual.

The running buffer (20 mmol/L HEPES at pH 7.5, 150 mmol/L NaCl, and 0.005% [*v/v*] Tween-20) was filtered through Millipore Film (pore size 0.22 mm) and degassed before use. The binding affinities were evaluated over a range of Rev7-3 (50–1600 nmol/L) and free Rev7 (0.4–12.8 μmol/L) concentrations at 25°C. Meanwhile, for both binding assays, the concentration of 400nmol/L was repeated as an internal control, and the free Rev3 was taken as a negative control. All of the data collected were analyzed using BIAevaluation software version 4.1.

Acceptor photobleaching FRET

FRET experiments were conducted as described by Chen et al (2009). Sequences encompassing Rev3[7BD] and Rev7-mKO were simultaneously cloned into a pcDNA vector (pcDNA[Rev3 and Rev7-mKO]). Similarly, sequences encompassing Polκ[RIR]-EGFP (residues 560–615) and Rev1[CTD] (residues 1130–1251) were simultaneously cloned into a pcDNA vector (pcDNA[Rev1 and Polκ-EGFP]). HEK-293T cells were co-transfected with pcDNA[Rev3 with Rev7-mKO] and pcDNA[Rev1 and Polκ-EGFP] as well as pcDNA[Rev3 and Rev7-mKO] and pcDNA[PolκRIR-EGFP]. We also transfected HEK-293T cells with EGFP fused with mKO (mKO-EGFP) as a positive control, and mKO-Rev7 and EGFP empty vector as a negative control. The FRET experiments were performed using a confocal microscope (FV1000; Olympus) equipped with 488 nm and 515 nm lasers. We used the sequence mode to prevent fluorescence leakage when capturing pre-photobleaching images. The acceptor (mKO) was then bleached by repetitive scanning of the cell with a full-power

515 nm laser for 4 min. Finally, with the same acquisition parameters as those applied to the pre-acceptor photobleaching images acquisition, the post-photobleaching images were acquired. The data were further analyzed using ImageJ software.

ADDENDUM

During the preparation of this manuscript, one paper on the crystal structure of human Rev3[7BD]-Rev7-Rev1 and another on mouse Rev3[7BD]-Rev7-Rev1[CTD]-Polk[RIR] were published online (Kikuchi et al., 2012; Wojtaszek et al., 2012a).

REFERENCES

Acharya, N., Haracska, L., Johnson, R.E., Unk, I., Prakash, S., and Prakash, L. (2005). Complex formation of yeast Rev1 and Rev7 proteins: a novel role for the polymerase-associated domain. Mol Cell Biol 25, 9734–9740.

Acharya, N., Johnson, R.E., Prakash, S., and Prakash, L. (2006). Complex formation with Rev1 enhances the proficiency of Saccharomyces cerevisiae DNA polymerase zeta for mismatch extension and for extension opposite from DNA lesions. Mol Cell Biol 26, 9555–9563.

Adams, P.D., Afonine, P.V., Bunkoczi, G., Chen, V.B., Davis, I.W., Echols, N., Headd, J.J., Hung, L.-W., Kapral, G.J., Grosse-Kunstleve, R.W., et al. (2010). PHENIX: a comprehensive Python-based system for macromolecular structure solution. Acta Crystallographica Section D 66, 213–221.

Alt, A., Lammens, K., Chiocchini, C., Lammens, A., Pieck, J.C., Kuch, D., Hopfner, K.-P., and Carell, T. (2007). Bypass of DNA lesions generated during anticancer treatment with cisplatin by DNA polymerase η. Science 318, 967–970.

Andersen, P.L., Xu, F., Ziola, B., McGregor, W.G., and Xiao, W. (2011). Sequential assembly of translesion DNA polymerases at UV-induced DNA damage sites. Mol Biol Cell 22, 2373–2383.

Auerbach, P.A., and Demple, B. (2010). Roles of Rev1, Pol zeta, Pol32 and Pol eta in the bypass of chromosomal abasic sites in Saccharomyces cerevisiae. Mutagenesis 25, 63–69.

Bienko, M., Green, C.M., Crosetto, N., Rudolf, F., Zapart, G., Coull, B., Kannouche, P., Wider, G., Peter, M., Lehmann, A.R., et al. (2005). Ubiquitin-binding domains in Y-family polymerases regulate translesion synthesis. Science 310, 1821–1824.

Biertümpfel, C., Zhao, Y., Kondo, Y., Ramón-Maiques, S., Gregory, M., Lee, J.Y., Masutani, C., Lehmann, A.R., Hanaoka, F., and

Yang, W. (2010). Structure and mechanism of human DNA polymerase [eegr]. Nature 465, 1044–1048.

Bomar, M.G., D'Souza, S., Bienko, M., Dikic, I., Walker, G.C., and Zhou, P. (2010). Unconventional ubiquitin recognition by the ubiquitin-binding motif within the Y family DNA polymerases ι and Rev1. Mol Cell 37, 408–417.

Chen, J., Ai, Y., Wang, J., Haracska, L., and Zhuang, Z. (2010). Chemically ubiquitylated PCNA as a probe for eukaryotic translesion DNA synthesis. Nat Chem Biol 6, 270–272.

Chen, Y., Deng, Y., Zhang, J., Yang, L., Xie, X., and Xu, T. (2009). GDI-1 preferably interacts with Rab10 in insulin-stimulated GLUT4 translocation. Biochemical J 422, 229–235.

Collaborative Computational Project, Number 4. (1994). The CCP4 suite: programs for protein crystallography. Acta Crystallogr D Biol Crystallogr 50, 760–763.

Doles, J., Oliver, T.G., Cameron, E.R., Hsu, G., Jacks, T., Walker, G.C., and Hemann, M.T. (2010). Suppression of Rev3, the catalytic subunit of Polζ, sensitizes drug-resistant lung tumors to chemotherapy. Proc Natl Acad Sci U S A 107, 20786–91

Dumstorf, C.A., Mukhopadhyay, S., Krishnan, E., Haribabu, B., and McGregor, W.G. (2009). REV1 is implicated in the development of carcinogen-induced lung cancer. Mol Cancer Res 7, 247–254.

Edmunds, C.E., Simpson, L.J., and Sale, J.E. (2008). PCNA ubiquitination and REV1 define temporally distinct mechanisms for controlling translesion synthesis in the avian cell line DT40. Mol Cell 30, 519–529.

Emsley, P., and Cowtan, K. (2004). Coot: model-building tools for molecular graphics. Acta Crystallogr D Biol Crystallogr 60, 2126–2132.

Freudenthal, B.D., Gakhar, L., Ramaswamy, S., and Washington, M.T. (2010). Structure of monoubiquitinated PCNA and implications for translesion synthesis and DNA polymerase exchange. Nat Struct Mol Biol 17, 479–484.

Friedberg, E.C., Lehmann, A.R., and Fuchs, R.P.P. (2005). Trading places: how do DNA polymerases switch during translesion DNA synthesis? Mol Cell 18, 499–505.

Gan, G.N., Wittschieben, J.P., Wittschieben, B.O., and Wood, R.D. (2008). DNA polymerase zeta (pol zeta) in higher eukaryotes. Cell Res 18, 174–183.

Garg, P., Stith, C.M., Majka, J., and Burgers, P.M. (2005). Proliferating cell nuclear antigen promotes translesion synthesis by DNA polymerase zeta. J Biol Chem 280, 23446–23450.

Goodman, M.F. (2002). Error-prone repair DNA polymerases in prokaryotes and eukaryotes. Annu Rev Biochem 71, 17–50.

Guo, C., Fischhaber, P.L., Luk-Paszyc, M.J., Masuda, Y., Zhou, J., Kamiya, K., Kisker, C., and Friedberg, E.C. (2003). Mouse Rev1 protein interacts with multiple DNA polymerases involved in translesion DNA synthesis. EMBO J 22, 6621–6630.

Guo, C., Kosarek-Stancel, J., Tang, T.-S., and Friedberg, E. (2009). Y-family DNA polymerases in mammalian cells. Cell Mol Life Sci 66, 2363–2381.

Guo, C., Sonoda, E., Tang, T.-S., Parker, J.L., Bielen, A.B., Takeda, S., Ulrich, H.D., and Friedberg, E.C. (2006). REV1 protein interacts with PCNA: significance of the REV1 BRCT domain in vitro and in vivo. Mol Cell 23, 265–271.

Guo, D., Wu, X., Rajpal, D.K., Taylor, J.S., and Wang, Z. (2001). Translesion synthesis by yeast DNA polymerase zeta from

templates containing lesions of ultraviolet radiation and acetylaminofluorene. Nucleic Acids Res 29, 2875–2883.

Hara, K., Hashimoto, H., Murakumo, Y., Kobayashi, S., Kogame, T., Unzai, S., Akashi, S., Takeda, S., Shimizu, T., and Sato, M. (2010). Crystal structure of human REV7 in complex with a human REV3 fragment and structural implication of the interaction between DNA polymerase ζ and REV1. J Biol Chem 285, 12299–12307.

Hoege, C., Pfander, B., Moldovan, G.-L., Pyrowolakis, G., and Jentsch, S. (2002). RAD6-dependent DNA repair is linked to modification of PCNA by ubiquitin and SUMO. Nature 419, 135–141.

Ito, W., Yokoi, M., Sakayoshi, N., Sakurai, Y., Akagi, J.-i., Mitani, H., and Hanaoka, F. (2012). Stalled Polη at its cognate substrate initiates an alternative translesion synthesis pathway via interaction with REV1. Genes Cells 17, 98–108.

Janda, C.Y., Li, J., Oubridge, C., Hernandez, H., Robinson, C.V., and Nagai, K. (2010). Recognition of a signal peptide by the signal recognition particle. Nature, 465, 507–510.

Kikuchi, S., Hara, K., Shimizu, T., Sato, M., and Hashimoto, H. (2012). Structural basis of recruitment of DNA polymerase ζ by interaction between REV1 and REV7. J Biol Chem 287, 33847–33852.

Kim, H., Yang, K., Dejsuphong, D., and D'Andrea, A.D. (2012). Regulation of Rev1 by the Fanconi anemia core complex. Nat Struct Mol Biol 19, 164–170.

Kosarek, J.N., Woodruff, R.V., Rivera-Begeman, A., Guo, C., D'Souza, S., Koonin, E.V., Walker, G.C., and Friedberg, E.C. (2008). Comparative analysis of in vivo interactions between Rev1 protein and other Y-family DNA polymerases in animals and yeasts. DNA Repair 7, 439–451.

Lawrence, C.W., and Hinkle, D.C. (1996). DNA polymerase zeta and the control of DNA damage induced mutagenesis in eukaryotes. Cancer Surv 28, 21–31.

Lehmann, A.R., Niimi, A., Ogi, T., Brown, S., Sabbioneda, S., Wing, J.F., Kannouche, P.L., and Green, C.M. (2007). Translesion synthesis: Y-family polymerases and the polymerase switch. DNA Repair 6, 891–899.

Lin, X., Okuda, T., Trang, J., and Howell, S.B. (2006). Human REV1 modulates the cytotoxicity and mutagenicity of cisplatin in human ovarian carcinoma cells. Mol Pharmacol 69, 1748–1754.

Livneh, Z., Z, O., and Shachar, S. (2010). Multiple two-polymerase mechanisms in mammalian translesion DNA synthesis. Cell Cycle 9, 729–735.

Mapelli, M., Massimiliano, L., Santaguida, S., and Musacchio, A. (2007). The Mad2 conformational dimer: structure and implications for the spindle assembly checkpoint. Cell 131, 730–743.

Masuda, Y., Ohmae, M., Masuda, K., and Kamiya, K. (2003). Structure and enzymatic properties of a stable complex of the human REV1 and REV7 proteins. J Biol Chem 278, 12356–12360.

Murakumo, Y., Ogura, Y., Ishii, H., Numata, S., Ichihara, M., Croce, C.M., Fishel, R., and Takahashi, M. (2001). Interactions in the error-prone postreplication repair proteins hREV1, hREV3, and hREV7. J Biol Chem 276, 35644–35651.

Murshudov, G.N., Vagin, A.A., and Dodson, E.J. (1997). Refinement of macromolecular structures by the maximum-likelihood method. Acta Crystallogr D Biol Crystallogr 53, 240–255.

Nair, D.T., Johnson, R.E., Prakash, L., Prakash, S., and Aggarwal, A.K. (2005). Rev1 employs a novel mechanism of DNA synthesis using a protein template. Science 309, 2219–2222.

Nair, D.T., Johnson, R.E., Prakash, S., Prakash, L., and Aggarwal, A.K. (2004). Replication by human DNA polymerase-[iota] occurs by Hoogsteen base-pairing. Nature 430, 377–380.

Ohashi, E., Hanafusa, T., Kamei, K., Song, I., Tomida, J., Hashimoto, H., Vaziri, C., and Ohmori, H. (2009). Identification of a novel REV1-interacting motif necessary for DNA polymerase κ function. Genes Cells 14, 101–111.

Ohashi, E., Murakumo, Y., Kanjo, N., Akagi, J.-i., Masutani, C., Hanaoka, F., and Ohmori, H. (2004). Interaction of hREV1 with three human Y-family DNA polymerases. Genes Cells 9, 523–531.

Okada, T., Sonoda, E., Yoshimura, M., Kawano, Y., Saya, H., Kohzaki, M., and Takeda, S. (2005). Multiple roles of vertebrate REV genes in DNA repair and recombination. Mol Cell Biol 25, 6103–6111.

Otwinowski, Z., and Minor, W. (1997). Processing of X-ray diffraction data collected in oscillation mode. In (Elsevier), pp. 307–326.

Plosky, B.S., Vidal, A.E., de Henestrosa, A.R.F., McLenigan, M.P., McDonald, J.P., Mead, S., and Woodgate, R. (2006). Controlling the subcellular localization of DNA polymerases [iota] and [eta] via interactions with ubiquitin. EMBO J 25, 2847–2855.

Pozhidaeva A, P.Y., D'Souza S, Bezsonova I, Walker GC, Korzhnev DM (2012). NMR structure and dynamics of the C-terminal domain from human Rev1 and its complex with Rev1 interacting region of DNA polymerase η. Biochemistry 51, 5506–5520.

Prakash, S., Johnson, R.E., and Prakash, L. (2005). Eukaryotic translesion synthesis DNA polymerases: specificity of structure and function. Annu Rev Biochem 74, 317–353.

Räschle, M., Knipscheer, P., Enoiu, M., Angelov, T., Sun, J., Griffith, J.D., Ellenberger, T.E., Schärer, O.D., and Walter, J.C. (2008). Mechanism of replication-coupled DNA interstrand crosslink repair. Cell 134, 969–980.

Sale, J.E., Lehmann, A.R., and Woodgate, R. (2012). Y-family DNA polymerases and their role in tolerance of cellular DNA damage. Nat Rev Mol Cell Biol 13, 141–152.

Shachar, S., Ziv, O., Avkin, S., Adar, S., Wittschieben, J., Reiszner, T., Chaney, S., Friedberg, E.C., Wang, Z., Carell, T., et al. (2009). Two-polymerase mechanisms dictate error-free and error-prone translesion DNA synthesis in mammals. EMBO J 28, 383–393.

Sharma, S., Hicks, J.K., Chute, C.L., Brennan, J.R., Ahn, J.-Y., Glover, T.W., and Canman, C.E. (2011). REV1 and polymerase ζ facilitate homologous recombination repair. Nucleic Acids Res 40, 682–691.

Uljon, S.N., Johnson, R.E., Edwards, T.A., Prakash, S., Prakash, L., and Aggarwal, A.K. (2004). Crystal structure of the catalytic core of human DNA polymerase dappa. Structure 12, 1395–1404.

Wojtaszek, J., Lee, C.J., D'Souza, S., Minesinger, B., Kim, H., D'Andrea, A.D., Walker, G.C., and Zhou, P. (2012a). Structural basis of Rev1-mediated assembly of a quaternary vertebrate translesion polymerase complex consisting of Rev1, heterodimeric Pol ζ and Pol κ. J Biol Chem 287, 33836–33846.

Wojtaszek, J., Liu, J., D'Souza, S., Wang, S., Xue, Y., Walker, G.C., and Zhou, P. (2012b). Multifaceted recognition of vertebrate Rev1 by translesion polymerases ζ and κ. J Biol Chem 287, 26400–26408.

Xie, K., Doles, J., Hemann, M.T., and Walker, G.C. (2010).

Error-prone translesion synthesis mediates acquired chemoresistance. Proc Natl Acad Sci U S A 107, 20792–20797.

Zhu, F., and Zhang, M. (2003). DNA polymerase zeta: new insight into eukaryotic mutagenesis and mammalian embryonic development. World J Gastroenterol 9, 1165–1169.